Title: The effect of high-pressure on organocatalyzed ROP of γ-butyrolactone

Author: Roksana Bernat, Paulina Maksym, Magdalena Tarnacka, Kajetan Koperwas, Justyna Knapik-Kowalczuk, Katarzyna Malarz, Anna Mrozek-Wilczkiewicz, Andrzej Dzienia, Tadeusz Biela, Roman Turczyn, Luiza Orszulak, Barbara Hachuła, Marian Paluch, Kamil Kamiński

Citation style: Bernat Roksana, Maksym Paulina, Tarnacka Magdalena, Koperwas Kajetan, Knapik-Kowalczuk Justyna, Malarz Katarzyna, Mrozek-Wilczkiewicz Anna, Dzienia Andrzej, Biela Tadeusz, Turczyn Roman, Orszulak Luiza, Hachuła Barbara, Paluch Marian, Kamiński Kamil. (2021). The effect of high-pressure on organocatalyzed ROP of γ-butyrolactone. „Polymer (Guildf.)" (2021, vol. 233, art. no. 124166, s. 1-14), DOI:10.1016/j.polymer.2021.124166

Polymer 233 (2021) 124166

Contents lists available at ScienceDirect

Polymer

journal homepage: www.elsevier.com/locate/polymer

The effect of high-pressure on organocatalyzed ROP of γ-butyrolactone

Roksana Bernat [a,b], Paulina Maksym [b,c,*], Magdalena Tarnacka [b,c], Kajetan Koperwas [b,c], Justyna Knapik-Kowalczuk [b,c], Katarzyna Malarz [b,c], Anna Mrozek-Wilczkiewicz [b,c], Andrzej Dzienia [b,d], Tadeusz Biela [e], Roman Turczyn [f], Luiza Orszulak [a], Barbara Hachuła [a,b], Marian Paluch [b,c], Kamil Kamiński [b,c]

[a] Institute of Chemistry, University of Silesia, Szkolna 9, 40-007, Katowice, Poland
[b] Silesian Centre for Education and Interdisciplinary Research, University of Silesia, 75 Pulku Piechoty 1A, 41-500, Chorzów, Poland
[c] Chelkowski Institute of Physics, University of Silesia in Katowice, 75 Pułku Piechoty 1, 41-500, Chorzów, Poland
[d] Institute of Materials Engineering, University of Silesia, 40-007, Katowice, Poland
[e] Department of Polymer Chemistry, Centre of Molecular and Macromolecular Studies, Polish Academy of Sciences, Sienkiewicza 112, 90-363, Lodz, Poland
[f] Department of Physical Chemistry and Technology of Polymers, Faculty of Chemistry, Silesian University of Technology, Strzody 9, 44-100, Gliwice, Poland

ARTICLE INFO

Keywords:
Ring-opening polymerization
PGBL
High-presssure

ABSTRACT

In this paper, we report 1,5,7-Triazabicyclo[4.4.0]dec-5-ene (TBD) supported high-pressure approach enforcing Ring-Opening Polymerization (ROP) of γ-butyrolactone (GBL), that due to unfavorable thermodynamics and low ring strain, is considered as a hardly polymerizable monomer. Application of Broadband Dielectric Spectroscopy (BDS) allowed us to find optimal thermodynamic conditions to perform well-controlled and notably fast polymerization (even within 1 h!), avoiding undesired crystallization process. It was shown that by varying pressure and temperature conditions, we could control molecular weight, dispersity of recovered macromolecules, as well as rate and efficiency of the reaction that are significantly altered with respect to the reference process carried out at ambient conditions. Experiments performed at respectively very low temperature $T = 233$ K and low/moderate pressure ($p = 75$–250 MPa) and much higher temperatures ($T = 248$–268 K) and compressions ($p = 1000$ MPa) yielded poly(γ-butyrolactone) (PGBL) of tailored absolute molecular weight in moderate range $M_n = 2.8$–15.0 (up to 30.3) kg/mol and narrow/moderate dispersity ranging from $Đ = 1.12$–1.89. What is more, the implementation of MALDI-TOF, GPC and DSC analyses, clearly indicated that as *i)* the time of reaction gets longer, *ii)* the amount of catalyst increases, *iii)* the temperature lowers, the content of cyclic products in produced polymers grows. This phenomenon influences the rheological properties (viscosity), foil formation ability (films) and cell culture proliferation features of the recovered macromolecules. Presented results open a highly effective and repeatable route to produce PGBL *via* pressure-assisted ROP and indicate the possibility of tuning properties of this polymer by varying concentration of cycles or eventual block copolymerization with other biorelevant monomers to meet the expectations of the biotechnological industry.

1. Introduction

The enormous demand for synthetic polymers/plastics led to the systematic growth of poorly recyclable and non-biodegradable wastes, contributing to the natural environment's increasing pollution. Better awareness of the threats connected to this problem enforced industry and researchers to search for new materials/replacements that are more eco-friendly and less harmful/neutral for living organisms. In this context, biodegradable and renewable polymers seem to be promising perspectives [1,2]. In fact, biodegradable, aliphatic polyesters that degrade chemically by hydrolytic cleavage are of particular interest [3]. Due to enhanced biocompatibility and thermoplastic properties, they have found many food industry applications, medicine and pharmacy [3], for example, in drug delivery systems [4–6], tissue engineering [7–9], implants [10–12], disposable food containers [13], and packaging materials [13].

Nevertheless, up to now, there are only a few polyesters, including synthetic ones as polylactide (PLA) or poly(ε-caprolactone) (PCL), as well as those produced by microbes [14] as polylactic acid and polyhydroxybutyrate (PHB) that are used in commercial applications.

* Corresponding author. Silesian Centre for Education and Interdisciplinary Research, University of Silesia, 75 Pulku Piechoty 1A, 41-500, Chorzów, Poland.
E-mail address: paulina.maksym@us.edu.pl (P. Maksym).

https://doi.org/10.1016/j.polymer.2021.124166
Received 2 July 2021; Received in revised form 2 September 2021; Accepted 5 September 2021
Available online 8 September 2021

Interestingly, the latter polymer is structurally identical to poly (γ-butyrolactone) (PGBL) that can be synthesized *via* the ring-opening polymerization (ROP) of γ-butyrolactone (GBL). Previous studies indicated that PGBL possesses numerous promising features such as the fastest rate of hydrolytic degradation (8–52 weeks [15]) among other polyesters [16,17] and interesting mechanical properties that can be tuned by the amount of (macro)cyclic forms of PGBL [18], making this polymer highly desirable biomaterial of the most truly biodegradable and renewable character. Unfortunately, due to unfavorable polymerization thermodynamics and kinetics, i.e., the positive Gibbs free energy [19] and strain in a very small GBL lactone ring, it is considered as *'hardly-polymerizable'* or even *'non-polymerizable'* monomer [20–22]. Consequently, despite the significant progress in the modern macromolecular chemistry toolbox, the production of PGBL remains a serious challenge. In fact, to date, only two research groups have successfully polymerized GBL in a controlled manner but at an extremely low-temperature range (233–253 K) [18,22,23]. In those pioneering work, a synthetic strategy based on developing novel, more efficient initiating/catalytic systems including metalorganic (i.e., lanthanide, yttrium complexes) [18,22,23] and less-toxic organocatalytic ones (i.e., phosphazenes [24,25], the bicyclic guanidine derivative 1,5,7-triazabicyclo [4.4.0] dec-5-ene (TBD) [18], N-heterocyclic carbenes [26], N-heterocyclic olefins [27] and systems of ion pairs based on (thio)ureas and phosphazenes [28,29] or ureas and alkoxide [30]) were proposed. As a result, well-defined PGBLs in a wide range of molecular weight up to $M_n \leq 80.4$ kg/mol (relative to PS standards) with narrow to high dispersity ($Đ = 1.09$–2.92) and yield (≤ 0.60 g_{PGBL}/g_{GBL}) were produced [29]. However, when TBD was employed as a catalyst, it was impossible to obtain such breakthrough macromolecules parameters (M_n = 5.55–6.15 kg/mol; $Đ$ = 1.14–1.22; yield ≤ 0.33 g_{PGBL}/g_{GBL}) [18]. Herein, one can briefly remind that organic catalysis has become a powerful alternative to more traditional metal-based catalysts since they were successfully applied also in ROP of a wide range of monomers [31,32], including other lactones [33,34], epoxides [35,36], cyclic carbonates [37] and cyclic siloxanes [38,39]. Some of them, e.g., N-heterocyclic carbenes, also display extremely high activities in the ROP of lactide (achieving 88% monomer conversion in less than 25 s at ambient temperature with 0.5 mol% of catalyst) [40].

The synthetic route described above based on novel catalysts, although breaking, is by far the most convenient and explored way of modern chemistry. Nevertheless, it is often forgotten that similar or even better results can be obtained for the systems exposed to the *'external'* physical factors such as laser, light irradiation, ultrasounds, friction and compression [41]. These approaches allow dealing with less complex from the chemical point of view compositions where the amount of catalysts or solvent can be significantly reduced or even completely eliminated. Thus, materials of exceptional purity can be synthesized. Herein, it should be emphasized that elevated pressure is a very promising approach for different kinds of polymerizations since, upon compression, chain propagation and bimolecular chain termination reactions are enhanced and suppressed, respectively [42,43]. Moreover, many competitive reactions occurring during the main polymerization process, such as chain transfer or transesterification, are characterized by different activation volumes and profoundly affect polymer structure and properties (e.g., degrees of polymerization, chain branching). Therefore, fabrication of polymeric materials of better macromolecular properties and quality (i.e., much lower dispersity, controlled functionality, selectivity, stereoregularity and topology) up to ultra-high molecular weight products not achievable under atmospheric pressure is possible. Another promising opportunity that arises from applying the high pressure is an enhancement of the polymerizability of monomers considered as unreactive or hardly-polymerizable at atmospheric pressure conditions, including the less-activated ones (LAMs) or those sterically hindered. These effects result from manipulating the density, viscosity, intermolecular interactions, or eventually phase transitions and micro-separations that influence diffusivity, reaction equilibria, concentration gradient, heat and mass transfer and generally thermodynamics (increasing the ceiling temperature) of the polymerizing systems at elevated pressures. Interestingly, although pressure-related effects were investigated in the case of different kinds of free- or controlled-radical polymerizations, little attention was paid to studying the progress of ROP in lactones or lactides. Herein, it is worth noting only a few works, including two previous ones of some of our group where it was shown that compression allows obtaining ultra-pure PCL of well-defined structural properties [44,45]. On the other hand, only one paper devotes the high-pressure impact on the cationic acid-catalyzed GBL ROP [46]. However, in that report, the use of strong organic acids contributed to the unwanted partial degradation/uncontrolled hydrolysis of produced PGBL forming polymers of high dispersity and poor chain-end fidelity.

Herein, we present a promising organocatalyzed high-pressure approach to obtain tailored PGBL (Scheme 1).

We envisioned that such a combination might offer controlled GBL polymerization similarly to our previous reports concerning the high-pressure ROP of another cyclic ester, ε-caprolactone providing ultra-pure PCLs. The main aim of our investigation was to probe the effect of varied thermodynamic conditions (T, p) on GBL polymerizability, reaction rate and properties of final products. We demonstrated that elevated pressure (p = 75–1300 MPa) could force relatively fast (even within 1 h) GBL polymerization at lower and higher temperature range (233–268 K). As a result, it was possible to synthesize well-defined PGBLs in a moderate range of an absolute M_n (2.8–15.0, up to 30.3 kg/mol), narrow dispersity ($Đ$ = 1.12) and higher yields (0.17–0.69 g PGBL/1g GBL) compared to previous synthetic approaches using TBD organocatalyst [18]. We also examine the possibility to tune properties (for example viscosity, foil formation ability) of the polymers by further chain extension polymerization with rac-lactide. This experiment allowed us to produce a well-defined diblock copolymer. Noteworthy, by simply extending polymerization timeframes, we were able to control the structural and topological parameters of produced PGBLs (more or less content of cyclic units) that meaningly affect their wettability, toxicity, flexibility [47] as well as film-forming properties.

2. Materials and methods

2.1. Materials

All chemicals used were purchased from Sigma-Aldrich. γ-Butyrolactone (GBL) (≥99%) was used as received. 1,5,7-Triazabicyclo[4.4.0] dec-5-ene (TBD) (98%) was dried using a Schlenk line prior to use. Toluene (TOL) (anhydrous, 99.8%), dichloromethane (DCM) (anhydrous, 99.8%), benzyl alcohol (anhydrous, 99.8%) and 1-butanol (anhydrous, 99.8%) were purged by passing an inert gas through it for 15 min prior to use.

2.2. Procedures

2.2.1. Reaction mixture preparation

Typically, the reaction mixture was prepared as followed: GBL (1.5 mL, 19.514 mmol), toluene (in v/v ratio 1/1, 1/2 or 2/1)/dichloromethane (in v/v ratio 1/3) and TBD (13.6 mg, 0.098 mmol) were placed in a Schlenk flask with a magnetic stirring bar. The solution was purified from residual moisture by three freeze-pump-thaw cycles and purged under nitrogen. Then, the appropriate amount of initiator (benzyl alcohol or 1-butanol) was added to the mixture under inert gas flow.

Herein, it must be stressed that a fairly important factor in ionic polymerization is the proper selection of the solvent. When the solvent is selected, the polarity, solvent dielectric constant, hydrogen-bonding formation ability, phase transition temperatures, and specific solvation effects must be considered. Equally important is the ability to effectively dissolve all reactants by selected solvent, aggregation/non-aggregation tendency of actually growing species, and finally tuning initial

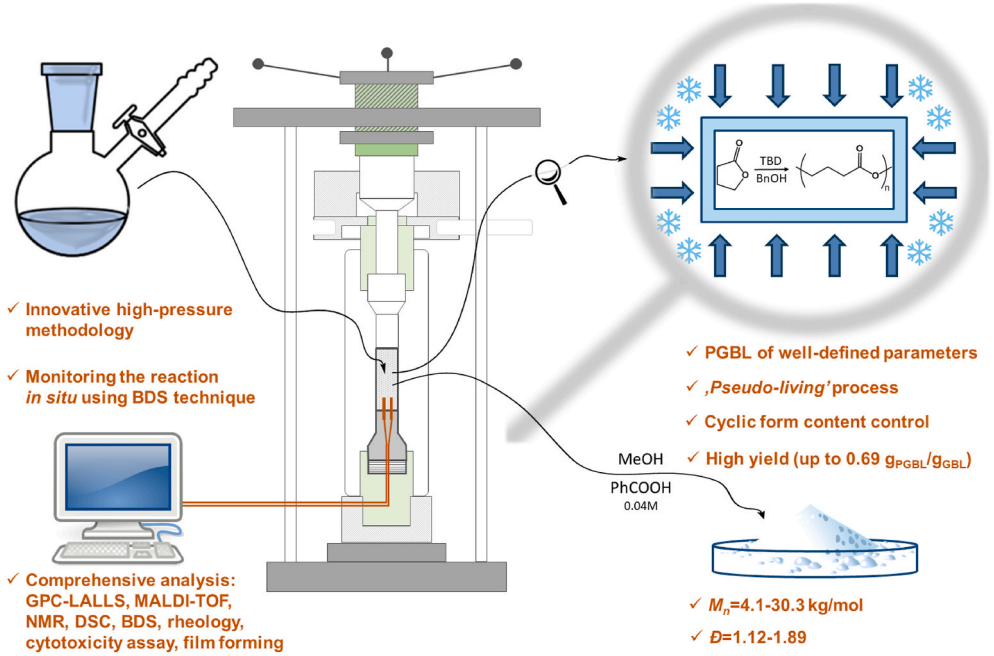

Scheme 1. Graphical scheme of the high-pressure strategy of PGBL production.

viscosity of the polymerization mixture. It should be mentioned that the polymerizing mixtures were consisted of two different solvents: toluene and dichloromethane. The choice was dictated by the fact that they have strong impact on the macromolecular properties of produced polyesters, the polymerization rate and the occurrence of transesterification reaction. DCM, being more polar, was successfully used together with TBD catalyst in a previous work of Hong et al. concerning low-temperature ROP of GBL [18]. In contrast, toluene is a non-polar solvent but is often used in the polymerization of other lactones [48,49]. Moreover, it is highly suitable for high-pressure-assisted syntheses. As mentioned, the acidity/basicity of selected solvents and their influence on the applied catalyst should also be taken into account. In particular, the similar basicity of TOL or DCM and catalyst can contribute to the competition in coordination with the hydroxyl initiating species or chain-end, which slows down the ROP process [50]. In addition, it should also be mentioned that TBD is a highly active unimolecular bifunctional catalyst for the ROP for lactide and lactones that could increase the rate of polymerization with a minimum amount of catalyst loading in non-polar solvents.

2.2.2. Ring-opening polymerization under high pressure

The Schlenk flask, together with PTFE tubes and pressure reactor, was moved to a glove-box filled with argon. Inert gas (Argon 5.0) was pumped through a Drierite™ gas-drying unit. Under inert and dry conditions, the reaction mixture was transferred to a PTFE ampoule closed with a metal cap, and then, the sealed Teflon ampoule was installed in the pressure reactor (LC10T, manufactured by Unipress – Institute of High Pressure Physics, Warsaw). Afterward, the pressure reactor was assembled, removed from the glove-box and left to cool in a thermostat to the set temperature. Subsequently, the pressure reactor was compressed by a hydraulic press (LCP20, Unipress) and placed in the thermostat again to adjust to the determined thermodynamic conditions for an appropriate time.

After the desired amount of time, the pressure was released as quickly as possible, and the post-reaction mixture was added to the 0.04 M benzoic acid/methanol solution to neutralize TBD and avoid the depolymerization of PGBL. Next, the precipitate of PGBL was filtered, washed with methanol and dissolved in a small portion of chloroform. Then a silica gel column was employed to purify the polymer and remove the remaining monomer. The polymer was isolated by precipitation into cold methanol, filtered and dried under vacuum to a constant mass.

The monomer conversion could not be determined by ^{1}H NMR because of the risk of depolymerization of PGBL. The reaction yield was assessed by gravimetric analysis. Purified PGBL was dissolved in THF to perform GPC-LALLS measurements.

2.3. Instruments

2.3.1. High pressure broadband dielectric measurements

The reaction mixture and high-pressure cell were prepared in the glove-box filled with argon to avoid contact with the air, oxygen and humidity. The dielectric cell with the liquid sample was placed into a Teflon bellow mounted in the high-pressure chamber. Hydrostatic pressure was generated by displacing the piston employing a hydraulic press. The pressure was measured by a Nova Swiss tensometric meter, which had an accuracy of 10 MPa. The temperature was controlled within 0.1 K by means of liquid flow from a thermostatic bath. The complex dielectric permittivity, $\varepsilon^*(\omega) = \varepsilon'(\omega) - i\varepsilon''(\omega)$, where ε' is the real part and ε'' is the imaginary part which is a function of frequency, were carried out using the Novocontrol Alpha dielectric spectrometer, over the frequency range from 10^{-2} to 10^6 Hz.

2.3.2. Differential scanning calorimetry (DSC)

Calorimetric measurements of the isothermal reaction were carried out by Mettler-Toledo DSC apparatus equipped with liquid nitrogen cooling accessory and an HSS8 ceramic sensor (heat flux sensor with 120 thermocouples). Temperature and enthalpy calibrations were performed by using indium and zinc standards. The polymeric samples were prepared in an open aluminum crucible (40 μL) outside the DSC apparatus and measured on heating from 243 K to 360 K at a constant heating rate of 10 K/min.

2.3.3. Nuclear magnetic resonance spectroscopy

Nuclear magnetic resonance (^{1}H and ^{13}C NMR) spectra were collected using a Bruker Ascend 500 MHz spectrometer for the samples in $CDCl_3$ as a solvent with TMS internal standard. Standard experimental conditions and the standard Bruker program were used.

2.3.4. Fourier transform infrared spectroscopy

The quality analysis of the samples was performed with IR spectroscopy. Fourier transform infrared spectroscopy (FTIR) measurements were carried out using a Nicolet iS50 FTIR spectrometer (Thermo Scientific) equipped with an attenuated total reflectance (ATR) mode setup in the spectral range of 4000 to 400 cm^{-1}. Spectra were measured by co-adding 32 scans for each spectrum at a 4 cm^{-1} resolution.

2.3.5. Gel permeation chromatography

Molecular weights and dispersities were determined by gel permeation chromatography (GPC) with Viscotek GPC Max VE 2001. Viscotek TDA 305 triple detection system (refractometer, viscosimeter, and low angle laser light scattering) was used for data collection and OmniSec 5.12 for processing. Two T6000 M general mixed columns were used for separation. The measurements were carried out in THF as the solvent at 303 K with a flow rate of 1 mL/min. The apparatus was used in a triple detection mode; hence the absolute molar mass (M_n and M_w) and the dispersity ($Đ$) were determined by triple detection. The dn/dc value has been determined for several polymers varying in M_n from a series of measurements of macromolecules concentration ranging from 0.002 to 0.01 g/mL.

2.3.6. Matrix-assisted laser desorption/ionization-time of flight spectroscopy

MALDI-TOF-MS experiments were performed on an Axima-Performance TOF spectrometer (Shimadzu Biotech, Manchester, UK), equipped with a nitrogen laser (337 nm). The pulsed extraction ion source accelerated the ions to the kinetic energy of 20 keV. All data were obtained in a positive-ion linear mode, applying the accumulation of 200 scans per spectrum. The linear-mode analysis's calibration was done using polyethylene glycol (PEG) in a mass range up to 8000 Da. The samples were dissolved in dichloromethane at a concentration of 6 mg/mL. The sample solutions were mixed with a 7 mg/mL matrix solution in the same solvent. Dithranol (1,8-dihydroxy-9,10-dihydroanthracen-9-one) was used as the matrix. KCl was dissolved in THF at a concentration of 6 mg/mL. The sample, matrix and KCl were then combined at a ratio of 20[thin space (1/6-em)]:[thin space (1/6-em)]10[thin space (1/6-em)]:[thin space (1/6-em)]1 v/v. Data were acquired in continuum mode until acceptable averaged data were obtained and were analyzed using a Shimadzu Biotech Launchpad program.

2.3.7. Rheological studies

The viscoelastic properties of produced PGBL and their copolymer were measured using ARES G2 Rheometer. The instrument was equipped with aluminum parallel plate geometry (diameter = 8 mm). Before the oscillation, temperature sweep rheological experiments, the samples were placed between the rheometer fixtures and heated up to 353 K. At this particular temperature, the examined materials were liquefied, and then the gap was set at ~1 mm. Next, the linear viscoelastic region was checked for each sample, and at appropriate strain value, the material's complex viscosity was examined in the frequencies from 1 to 100 Hz at temperatures from 353 to 303 K.

2.3.8. Scanning electron microscopy

The SEM images of PGBL specimens were recorded using Phenom Pro-X microscope equipped with high brightness LaB6 source and high sensitivity 4-segments BSE detector and fully integrated EDS detector from Thermo Fisher Scientific. The operation conditions were as follows: acceleration voltage 10 kV, a low-vacuum mode for non-coated samples.

2.3.9. Cell culture and cytotoxicity assay

The bioactivity of PGBL samples was tested on two normal cell lines: the normal human fibroblasts (NHDF) and the human osteoblasts (HOB). Commercially available cell lines were purchased from PromoCell. NHDF cells were growing in Dulbecco's Modified Eagle's Medium (DMEM) supplemented with 15% of non-inactivated fetal bovine serum (FBS; Sigma). HBO cell line was cultured in osteoblast growth medium (Sigma). The culture medium contained a standard mixture of antibiotics (1% v/v of penicillin and streptomycin; Gibco). The cells were grown under standard conditions at 310 K in a humidified atmosphere at 5% CO_2. All cell lines were tested using the PCR technique for mycoplasma contamination.

Tested materials were poured (in sterile conditions) on a 12-well plate directly before the main viability assay. Then tested cell lines were seeded at a density of 50 000 cells/well and incubated at standard growing conditions for 48 h. After this time, 200 μL CellTiter 96® AQueous One Solution - MTS (Promega) solution in 1 mL DMEM medium without phenol red and FBS was added to each well. After 1 h, the absorbance of the synthesized formazan (mitochondrial activity indicator) was measured at 490 nm. The obtained results are expressed as a percentage of the reference material – uncoated well. Each material was tested in three independent experiments.

2.3.10. Cell adhesion assay

Cells were seeded directly on studied materials at a density of 30 000 cells/cm^2 and incubated at 310 K for 48 h. Next, the culture medium was replaced by a 5 μM dye solution – CellTracker Green CMFDA and incubated at 310 K for 1 h. After incubation, PGBL samples with attached cells were washed three times with the medium without phenol red, and FBS and then the materials were transferred to a 35 mm imaging dish with a polymer coverslip. Visualization of cells was carried out using Zeiss AxioObserver Z1 inverted fluorescence microscope equipped with an AxioCam RMn camera.

3. Results and discussion

One can recall that recent studies on high-pressure ROP polymerization of ε-caprolactone have clearly shown that crystallization of compressed monomer/reaction mixture is the critical issue that strongly influences the progress of the polymerization process and properties of the synthesized polymers [44]. Therefore, finding optimal thermodynamics conditions to avoid this undesired process is important to gain control over the reaction and obtain well-defined macromolecules. Since our preliminary calorimetric measurements carried out for γ-butyrolactone at p = 0.1 MPa have clearly revealed its great tendency to crystallization at low temperatures irrespectively to the applied cooling rate (see Fig. S1 in SI file), it was quite obvious that this process might be enhanced at elevated pressure even for the highly diluted systems composed of catalyst, initiator and solvent. To monitor the effect of pressure on crystallization, we have applied broadband dielectric spectroscopy. In this study, we measured a variation of the static permittivity and evolution of the dielectric loss spectra of the polymerizing mixture upon compression and time-dependent investigations at different T and p. Representative dielectric dispersion (ε') and loss (ε") spectra of the polymerizing mixture (monomer:initiator:catalyst in the ratio $[GBL]_0/[BnOH]_0/[TBD]_0$ = 200/1/1 of different amount of solvent) measured at T = 243 K and T = 253 K at p = 1000 MPa are shown in Fig. S2 (see SI file).

Briefly (for a more extensive discussion of dielectric data, please see SI), as shown in Fig. S2ac, both the polymerization and the crystallization process induce more or less the same variation in dielectric constant (plateau at higher frequency range). In both cases, it drops with time. However, more noticeable changes are observed in dielectric loss spectra (Fig. S2bd). In the case of polymerization, we observe the relaxation process (called 'segmental' or 'α-process') that enters the experimental window and then moves to the lower frequencies with the progress of the reaction (Fig. S2d). The change in the maximum of this peak (relaxation time) is closely connected to the increasing viscosity of the polymerizing system due to the growing polymer chains. On the other hand, no such effects are noted for the crystallization process (Fig. S2b). Hence, the analysis of both real and imaginary parts of the complex permittivity is a useful tool to establish optimal conditions for

the polymerization where the crystallization can be avoided. What is more, our study clearly revealed that in order to avoid this undesired process one should either increase the temperature or lower the pressure. Therefore, a balance between these two thermodynamic variables must be found to carry out unperturbed high pressure ROP of γ-butyrolactone.

The analysis of the dielectric data measured at different thermodynamic conditions allowed us to conclude that at very low ($T = 233$ K) and higher ($T = 248$ K) temperatures, one can operate at $p = 250$ MPa or $p = 1000$ MPa, respectively, avoiding crystallization process at least at the time required for the polymerization to be finished.

Having in mind the results of our dielectric investigations and a recent report by Hong et al. [18], on the polymerization of GBL catalyzed by TBD, analogous high-pressure experiments at the same $T = 233$ K and molar ratios of the initiator/monomer/catalyst were carried out in two different solvents: toluene (entries S1–S28 Table S1 in SI) and dichloromethane (entries S29–S38, Table S1 in SI).

The molecular weight, dispersity as well as yield of polymer vs time of reaction performed at indicated thermodynamic conditions were presented in Fig. 1. It was found that at higher pressure, a linear increase in the yield, molecular weight and dispersity of the polymer is noted as the reaction proceeds. Nevertheless, the slight growth of the last parameter was still in the acceptable range allowing us to certify that well-defined PGBL can be obtained at selected thermodynamic conditions. It is also worth pointing out that at $p = 250$ MPa and $T = 233$ K, the polymerization of GBL was very fast, yielding a quite high amount of polymer of moderate M_n and low $Đ$ even after 1 h (the result that is not attainable for ambient pressure ROP of GBL catalyzed by TBD). In addition, the pressure dependence on M_n, $Đ$ and yield of obtained polymers for the syntheses carried out for 24 h using two solvents (DCM, TOL) under isothermal conditions ($T = 233$ K) was presented in Fig. S3 (please see SI). Briefly, a growing tendency for the M_n and yield together with increasing pressure can be observed in the case of both solvents. The toluene-mediated syntheses yielded polymers of narrow molecular weight distribution, while DCM-assisted ones resulted in moderate $Đ$ values. The other interesting observation worth commenting on is that DCM offers better progress of the polymerization process maintaining good properties of the polymers with respect to toluene. This finding can be easily explained, considering that the former solvent is more suitable for low-temperature reactions. What is more, one should also note that we observed a similar trend in both studied systems: growing dispersity with increased polymerization timeframe (see Fig. 1). Note that obtained polymers revealed similar dispersity values at the early stage of both processes ($Đ = 1.11$–1.13 for $t = 3$ h, see entries S17 and S32, Table S1 in SI). Moreover, the significant difference between $Đ$ was noted for processes that lasted 24 h. As presented in Fig. 1b, after 24 h, PGBL obtained within the DCM-assisted GBL ROP was characterized by a much higher dispersity value than the toluene-assisted process ($Đ = 1.30$ and $Đ = 1.08$, respectively). However, when the reaction time was extended up to 96 h, a significant increase in dispersity was also observed in the case of the system consisted of toluene as a solvent ($Đ = 1.40$, entry S23, Table S1 in SI), while for the DCM-mediated one the $Đ$ value remained at a similar level ($Đ = 1.26$, see entry S38, Table S1 in SI). What is more, for the DCM-assisted process, we observed a much higher yield of resulted PGBL (see Fig. 1c). On the other hand, molecular weights of PGBLs obtained for the reactions consisted of TOL were higher (see Fig. 1a). We assume that solvents' polarities and their acidity/basicity character could be responsible for such a pattern of behavior. The higher polarity of DCM could result in a much higher rate of both ring-opening and transesterification processes. Consequently, the polymerization conducted in DCM occurred with more activity but poorer control than toluene-mediated one, which was reflected in higher dispersity and yield of produced PGBL. It is also worth mentioning that DCM can react with primary, secondary and tertiary aliphatic amines [51], leading to generating amine salt. Moreover, besides secondary amine such as piperidine, DCM is capable of functioning with tertiary amine like pyridine [52]. Thus, one can suppose that the TBD (guanidine derivative) catalyst used in the examined system can also undergo the quaternization reaction in the presence of DCM. Consequently, the nature of the catalyst changes to more ionic, which may affect its activity. Increasing catalytic activity in DCM-mediated systems could result from their acidic character and further quaternization of TBD catalysts. Similar observation relevant to increasing catalyst activity was noted for phosphazene (t-BuP_2)-catalyzed ε-caprolactone ROP using DCM as a solvent [50]. The authors showed that process performed in less polar toluene was characterized by a lower rate but greater control than in DCM-mediated syntheses, which is consistent with our results.

In the next step, we probed the impact of the increasing temperature on the properties of the synthesized polymers. However, it was found that the efficiency of the polymerization systematically dropped. Therefore, to compensate the negative effect of temperature growth, we had to elevate the pressure up to $p = 1000$ MPa to keep the reaction parameters in the acceptable range. Hence, as a consequence, a series of high-pressure experiments ($p = 500$–1300 MPa) at different initial monomer:initiator ratio ($[GBL]_0/[I]_0 = 200/1$, $1000/1$), type of initiator (benzyl alcohol BnOH vs n-butanol), the monomer concentration (bulk, 4.34 M, 6.5 M, 8.67 M) and TBD concentration at following range of temperatures 248–268 K (please see Table 1 and Table S1 in SI) were conducted.

Initially, we have performed reactions at the most extreme conditions at $T = 243$ K and $p = 1000$ MPa. However, due to the weak reproducibility of these experiments, this data will be discussed in more detail in SI.

Having in mind both outcome of the dielectric studies and poor repeatability of the experiments at the most extreme conditions, further solvent-assisted polymerization (100% toluene in respect to GBL volume, [GBL] = 6.5 M) investigations were performed at $T = 258$–268 K where crystallization was completely suppressed at $p = 1000$ MPa, which seems to be optimal pressure at higher temperatures to maintain controlled progress of the polymerization avoiding undesired

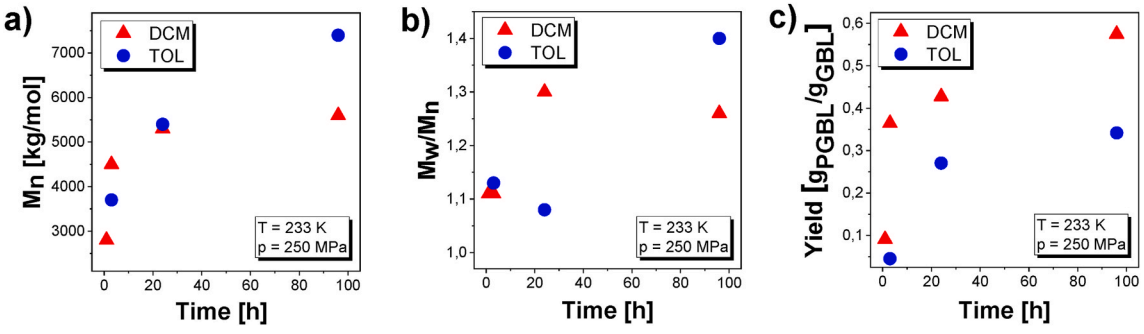

Fig. 1. The dependence of M_n **(a)**, $Đ$ **(b)** and yield **(c)** of PGBL vs time ($t = 1$ h; 3 h; 24 h; 96 h) of reactions carried out at $T = 233$ K and $p = 250$ MPa using different solvents. Based on: Table S1 in SI (TOL: entries **S17**, **S21**, **S23**; DCM: entries **S30**, **S32**, **S36**, **S38**).

Table 1
Reaction conditions and characteristics of PGBL synthesized under various thermodynamic conditions.

Sample no.	Time [h]	Pressure [MPa]	Temperature [K]	Monomer concentration [mol/L]	M_n[a] [g/mol]	Đ[a]	Yield [g_{PGBL}/g_{GBL}]
			$[GBL]_0/[BnOH]_0/[TBD]_0 = 1000/1/1$				
1	70	1000	258	6.5	30300	1.24	0.0206
			$[GBL]_0/[BnOH]_0/[TBD]_0 = 200/1/1$				
2	3	1000	248	6.5	6500	1.29	0.4411
3	24	1000	248	6.5	11400	1.30	0.5611
4	70	1000	248	6.5	7500	1.52	0.6263
5	57	1000	248	8.67	5700	1.68	0.4638
6	3	1000	253	6.5	7100	1.40	0.4440
7	1	1000	258	6.5	4100	1.15	0.1929
8	3	1000	258	6.5	7700	1.12	0.4747
9	5	1000	258	6.5	7500	1.21	0.4299
10	22	1000	258	6.5	5400	1.56	0.1727
11	70	1000	258	6.5	12000	1.42	0.5292
12	96	1000	258	6.5	15000	1.39	0.6945
13	3	1000	258	8.67	7500	1.43	0.4936
14	20	1000	263	8.67	7800	1.13	0.3633
15	3	1000	268	bulk	6700	1.35	0.1492
			$[GBL]_0/[BnOH]_0/[TBD]_0 = 1000/1/10$				
16	24	1000	253	6.5	8600	1.63	0.4012
17	72	1000	253	6.5	10400	1.89	0.4282

[a] Determined by GPC-LALLS (THF as an eluent). Estimated dn/dc = 0.066. Toluene as a solvent.

solidification of the polymerizing system. It was found that carrying out polymerization at $T = 258$ K and $p = 1000$ MPa allows the production of PGBL of the best structural parameters within 1–3 h ($M_n = 4.1$–7.7 kg/mol; $Đ = 1.12$–1.15, samples 7 and 8). However, in that case, the variation in the polymerization time led to a significant dispersity change (see Fig. 2a). Admittedly, as the feed ratio gradually increased from 200/1 to 1000/1 at $T = 258$ K and $p = 1000$ MPa, $[BnOH]_0/[TBD]_0 = 1/1$, we were able to produce PGBL od M_n reaching 30.3 kg/mol, $Đ = 1.24$; (sample 1) after 70 h but the efficiency of the reaction was very poor (0.02 g_{PGBL}/g_{GBL}). It is also worth mentioning the temperature effect on the M_n, $Đ$ and yield of obtained PGBLs for the reactions carried out for 3 h in toluene at $p = 1000$ MPa (see Fig. S4 in SI). Note that despite the linear growth of M_n with the temperature increase, the most effective polymerization process occurred at $T = 258$ K (the highest yield, the lowest $Đ$ value).

Within this work, we also performed reference reactions with n-butanol acting as initiator of the GBL ROP (entries S39–S42, Table S1 in SI). However, the reactions proceeded with poor control, yielding polymers of higher $Đ$ values ($Đ = 1.48$–1.69). Moreover, the reactions carried out at the same thermodynamic conditions using BnOH but with higher TBD concentration ($[GBL]_0/[BnOH]_0/[TBD]_0 = 200/1/2$, see entry S28, Table S1 in SI; and 1000/1/10, see entries 16–17, Table 1) also resulted in polymers of higher dispersity ($Đ = 3.2$ in case of the ratio: 200/1/2 and $Đ = 1.63$–1.89 in case of the ratio: 1000/1/10 of $[GBL]_0/[BnOH]_0/[TBD]_0$). It should be also mentioned that additional high-pressure solvent-assisted experiments ($p = 1000$ MPa) at $T = 273$ K and $T = 298$ K revealed no TBD activity. Besides the solvent-assisted experiments mentioned above, progress of bulk polymerization at $p = 1000$ MPa and $T = 268$ K (the temperature was selected to avoid GBL crystallization) was investigated. Interestingly, it was found that the polymerization occurred, delivering PGBL of $M_n = 6.7$ kg/mol and $Đ = 1.35$. However, it is worth pointing out that process's efficiency was low, yielding 0.15 g_{PGBL}/g_{GBL} within 3 h (sample 15). Noteworthy, further compression up to $p = 1300$ MPa and the addition of the solvent to the polymerizing system enhances both macromolecular characteristics ($M_n = 8.9$ kg/mol and $Đ = 1.36$) and the yield of polymer (0.52 g_{PGBL}/g_{GBL}, please see entry S13, Table S1 in SI). Finally, one should also emphasize that we were able to polymerize GBL at lower pressure $p = 500$ MPa at $T = 258$ K. Although we found this process quite effective (yield 0.3333 g_{PGBL}/g_{GBL}) and leading to the production of PGBL of $M_n = 2.8$ kg/mol, the reaction was not fully controlled as evidenced by dispersity $Đ = 2.6$ (please see entry S8, Table S1 in SI).

The structure of the produced PGBL with the successful incorporation of initiator moiety into polymer backbone has been confirmed by the ^{1}H NMR, ^{13}C NMR, FTIR and MALDI-TOF analysis. The representative ^{1}H and ^{13}C NMR spectra of produced PGBLs are presented in Fig. 3 (note the peaks of $\delta = 3.50$; 3.71; 5.14; 7.38 (a) and $\delta = 61.91$; 128.35 (b) originated from the end groups of the initiator - benzyl alcohol; and peaks of $\delta = 1.98$; 2.41; 4.13 (a) and $\delta = 24.05$; 30.51; 63.6 (b) being a confirmation of the presence of $–CH_2$ groups of PGBL units).

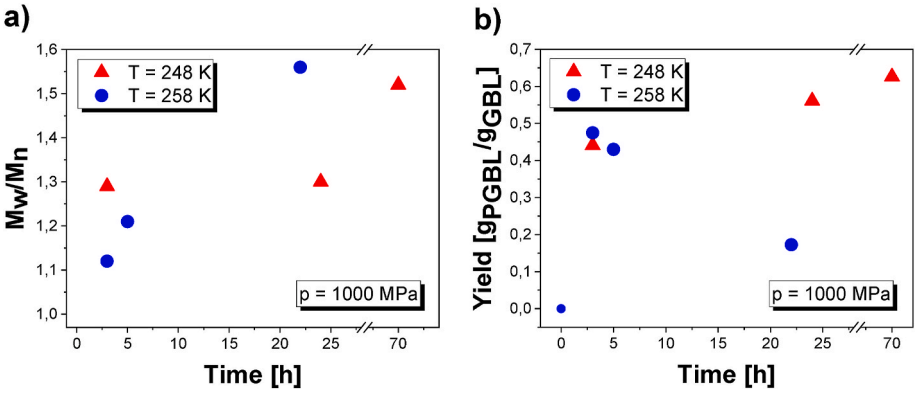

Fig. 2. The dependence of $Đ$ **(a)** and yield **(b)** vs time ($t = 3$ h; 5 h; 22 h; 24 h; 70 h) of PGBL produced at $T = 248$ K and $T = 258$ K ($p = 1000$ MPa). Based on the Table 1 ($T = 248$ K: entries **2–4**; $T = 258$ K: entries **8–10**).

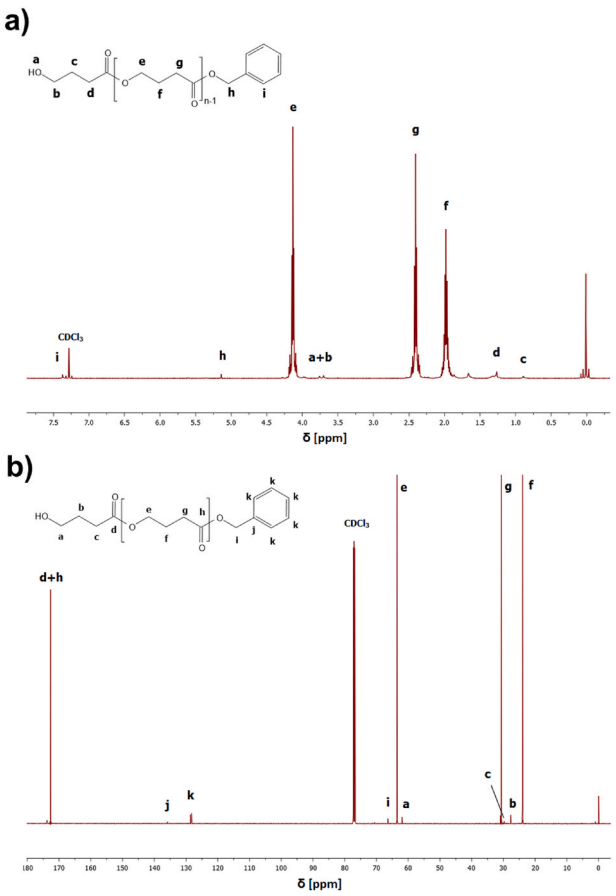

Fig. 3. ^{1}H NMR (a) and ^{13}C NMR (b) spectra of produced PGBL (**sample 8**).

Within this work, we also performed a chain extension experiment with rac-lactide to gain insight into the 'pseudo-livingness' of the studied herein system (please see ^{1}H and ^{13}C NMR and FTIR analysis in SI, Figs. S5 and S6, respectively). As a result, a well-defined PGBL-bl-PLA diblock copolymer was produced. It should be mentioned that diblock copolyesters based on PGBL and PLLA were recently reported to be successfully prepared via one-pot sequential ROP in the presence of cyclic trimeric phosphazene base (CTPB) as a catalyst [53].

In the next step, we carried out GPC investigations on the recovered polymers. These studies clearly revealed well-defined properties of PGBL produced via high-pressure TBD-mediated experiments in the range of T = 248–268 K reflected by the symmetric and monomodal shape of the GPC-LALLS traces (Fig. 4). Chromatograms of PGBL together with diblock copolymer PGBL-bl-PLA were presented in Fig. S7 in SI. Herein it must be stressed that dn/dc value has been determined for several polymers varying in M_n from a series of measurements where macromolecules concentration was changed. Importantly, this parameter remained constant (within experimental uncertainty) irrespectively of the sample. Interestingly, these chromatograms got broader while extending the reaction timeframe or decreasing temperature (T = 248 K) (Fig. 4).

This phenomenon can be interpreted as due to the increasing content of the cyclic polymers being side products of GBL ROP. The formation of macrocyclic structures aside from the linear polyester macromolecules is a quite common scenario in the ring-opening polymerization process. Intra- and intermolecular transesterification side reactions between propagating polymer chains lead to obtaining macrocyclic forms or oligomeric products, respectively. Thus, in each polymerization process, one can also identify cyclic polyesters in the recovered polymers. Interestingly, it seems that the content of cyclic side products decreases with pressure, as we mentioned in a previous paper of our group concerning TBD catalyzed ROP of ε-caprolactone [45]. It indicates that side reactions are strongly suppressed in the more viscous and dense polymerizing mixture. It can be explained by the fact that at these conditions, the diffusion of the monomer to the active centers is easier than the diffusion of much bigger polymer segments. It is consistent with the literature data where the termination and transesterification reactions are considered to be diffusion-controlled processes. At this point, it is worth mentioning that cyclic polymers, due to their different structural shape, are characterized by much different hydrodynamic radius, a radius of gyration with respect to their linear counterparts having similar molecular weights. As a consequence, the behavior of these materials on the chromatographic columns can be much different. In this context, one can remind recent studies demonstrating that cyclic polymers tend to be eluted at higher retention times with increasing molecular weight in contrast to the linear macromolecules. Nevertheless, cyclic polymers can be easily detected by the more detailed analysis of the collected chromatograms, especially the baseline's position on the right side of the RI detector response peak. In panels a and b of Fig. 4, we presented representative GPC traces where a clear change in baseline at higher retention times related to the response coming from cyclic moieties is noted. Considering that the RI detector is usually used to measure the total and temporary concentration of eluted polymer, these data can be used to determine the concentration of both linear and cyclic polymer fractions. It is possible since the polymerization process is controlled, which translates into modeling the RI detector response using the Gauss distribution function. This procedure is well illustrated in Panel C in Fig. 4 (the rest of the fitted experimental data can be found in Fig. S8, SI). The linear and cyclic fraction content has been calculated, considering that the RI detector response peak area for linear and cyclic polymers is proportional to the analyzed polymer sample concentration. The procedure of the calculations was described in more detail in SI. Furthermore, we assumed the dn/dc parameter to be constant (as we obtained from previous measurements) for both polymer fractions. As a consequence of the assumptions mentioned above, it was found that as the reaction time gets longer, the content of cyclic moieties increases from below 1% for sample 2 through 2.5% for sample 4 up to 5% for sample 3. Moreover, for the systems with high catalyst content, as in sample 17, the cyclic fraction concentration increases even up to 10%. Unfortunately, we could not calculate the molecular weight of cyclic polymers from our analysis because of the low sensitivity of the LALLS detector for low-molecular-weight compounds, which dominate in cyclic polymer fractions.

Aside from the routine NMR and GPC analysis, we also performed further MALDI-TOF studies on the PGBL produced at different thermodynamic conditions to gain insight into the impact of the 'external' conditions and polymerization time on the occurrence of the side reactions and population of the linear and cyclic products of ROP. It should be mentioned that the divergence in the molecular weight values determined using GPC and MALDI-TOF may be observed as a consequence of the different tendency to fragmentation of the polymer fraction of higher and lower molecular weight. The raw data obtained from MALDI-TOF were processed by setting an intensity threshold at 2% and removing artificially intense, low m/z peaks derived from the ionization of the matrix. The resulting spectra were then deconvoluted (for comparing raw and processed MALDI-TOF spectra, please see Fig. S9 in SI). Next, according to the end groups' weight, the peaks were assigned to the three corresponding data series (see Figs. S10 and S11 in SI) compiled in Fig. 5.

The MALDI-TOF analyses carried out for four representative samples, produced using different initial monomer/initiator/catalyst ratios and differing in polymerization times, confirmed the GBL monomer unit's weight equal to 86.09. One can add that this value was used for subsequent calculations of theoretical molecular weights M_{calc} according to the formulas given below in Table S2 (SI). Furthermore, good compliance of experimentally obtained molecular weights – M_{exp} with respective theoretical values M_{calc} (characterized by the difference

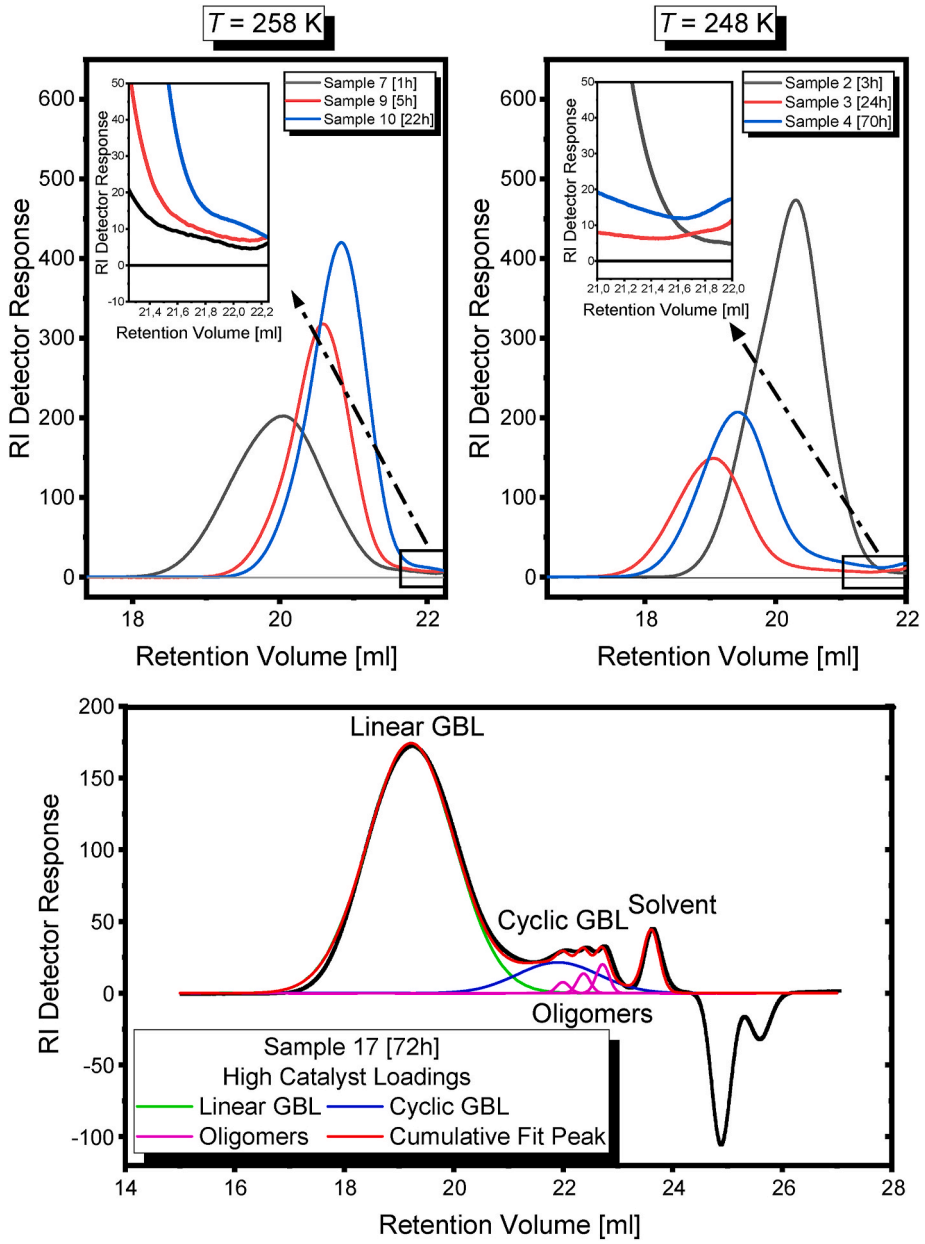

Fig. 4. GPC-LALLS traces of PGBL samples produced within different reaction times at: panel a) $T = 248$ K and panel b) $T = 258$ K. Panel c) Modeling of RI Detector Response with multiple Gaussian functions.

between these two parameters lower than two units, Fig. S11 and Table S2) allows confirming the chemical structure of PGBL synthesized at high-pressure ROP.

As we move towards the main part of the analysis, it needs to be emphasized that the efficiency of molecular weight control in ROP reactions depends on several factors, including reaction kinetics ($k_{propagation}/k_{initiation}$), an occurrence of intra- and intermolecular transesterification side reactions (leading to macrocyclic structures, shorter chains or chain redistributions), and the polymerization-depolymerization equilibrium. Obviously, all of these factors result in polymers with higher dispersity. Their extent depends on the ROP thermodynamical conditions, the reaction mixture's composition, polymerization time and the catalyst neutralization method.

Nevertheless, the analysis of the recorded spectra allows us to conclude that there are three main series of peaks, related to the i) potassium adducts of linear polymer with benzyl ester as a chain ends being a result of the main GBL ring-opening reaction (BnOOC- γBL-H + K^+, marked with red color) ii) potassium adducts of linear polymer terminated with methyl ester that resulted from transesterification reaction occurring during PGBL neutralization procedure (MeOOC-γBL-H + K^+, marked with green color), and iii) cyclic products of intramolecular transesterification reactions in the measured samples (cyclic γBL + K^+, marked with blue color) (for structures, please see Fig. S10 in SI). The processed spectra were then compiled in Fig. 5 and used for our further discussions. It is also worth noting that the molecular weights recorded on MALDI-TOF are lower than those measured using GPC-LALLS, consistent with our previous observations for other lactones [44,45].

Differences in the spectrograms given in Fig. 5 are particularly evident between samples 8, 14 and 16, 17. All these polymers were prepared under 1000 MPa but at different temperatures and timeframes, as follows: $T = 258$ K within 3 h, $T = 263$ K within 20 h, $T = 253$ K within 24 h, $T = 253$ K within 72 h for samples 8, 14, 16 and 17, respectively. In addition, both latter reactions were performed with much higher

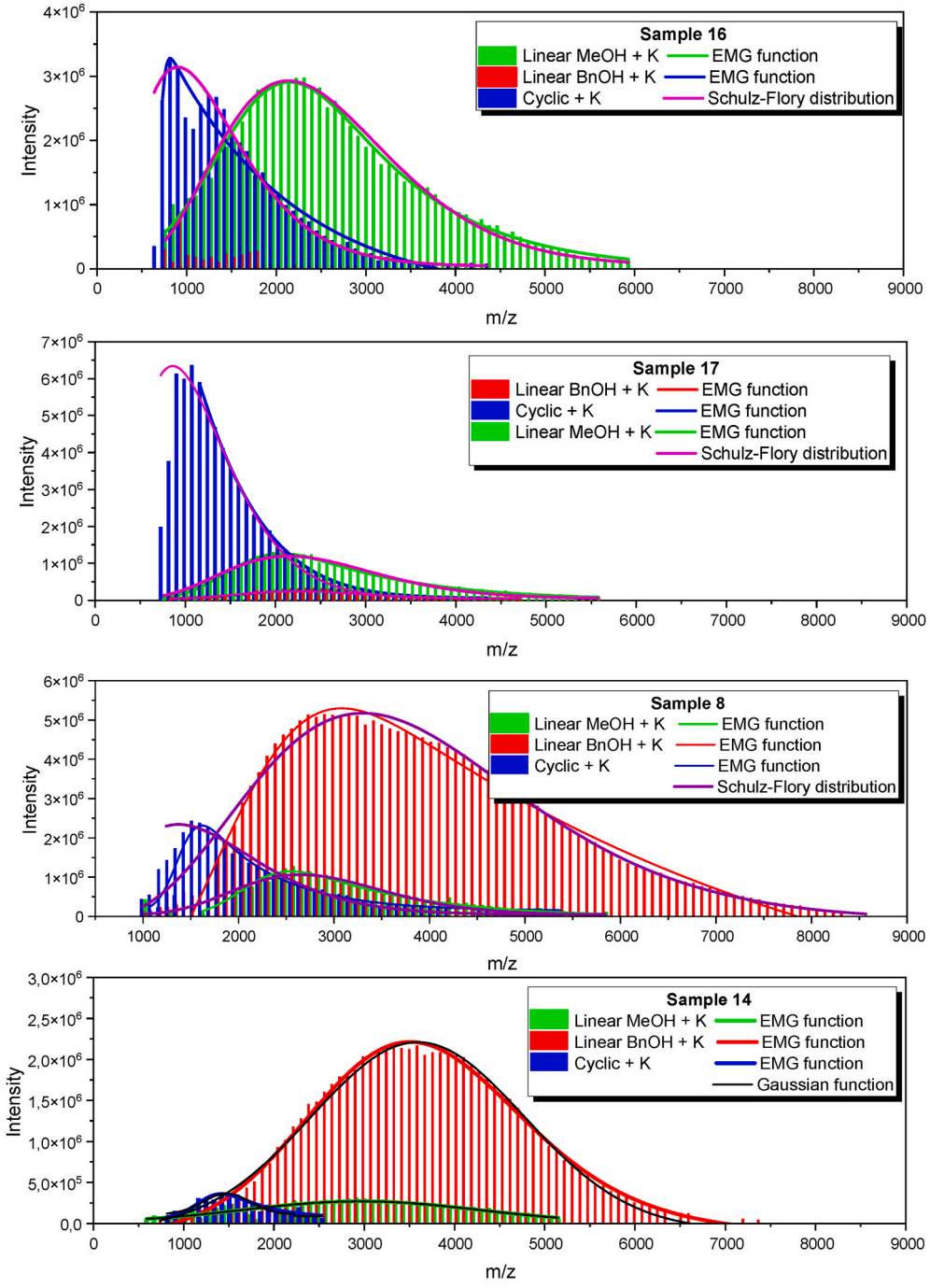

Fig. 5. MALDI-TOF mass spectrum of samples 16, 17, 8, 14 recorded in linear mode.

monomer and TBD concentration compared to the other samples ($[GBL]_0/[BnOH]_0/[TBD]_0$ = 1000/1/10 vs 200/1/1). Although we cannot indicate which of these factors is predominant, it is obvious that a higher content of cyclic products characterizes polymers prepared at higher catalyst content, lower temperature and within prolonged reaction time. Referring to the analysis of the MALDI-TOF mass spectra of PGBL obtained at higher TBD concentration (samples 16 and 17), dominant structures are cyclic products that result from, as we assume, a higher depolymerization rate. We suppose that this factor influences the polymerization-depolymerization equilibrium that could intensify the formation of cyclic products as a particular case of intramolecular transesterification processes. Contrary, spectra of samples produced at lower TBD content (samples 8 and 14) reveal a much lower intense series of cyclic polymers. Furthermore, the temperature of the polymerization may be crucial for the contribution of cyclic polymers, which for samples 16 and 17 was equal to $T = 253$ K. This conclusion can be confirmed by the relatively small amount of cyclic polymers for sample 14 ($T = 263$K), which, despite similar, long reaction time to the sample 16, is characterized by a much smaller amount of side products of the cyclization reaction. However, in that case, it is also necessary to take into account the much lower catalyst concentration influencing the overall polymerization path and properties of final polymers. Also, the method of neutralization of the reaction mixture is quite important for the polymer chain structure. In this context, it is worth comparing samples 16 and 17, which were neutralized with a very diluted solution of strong hydrochloric acid in methanol, with samples 8 and 14

neutralized with an 0.04 M methanolic solution of weak benzoic acid. In the former case, the dominant series of linear polymers terminated with methyl ester (coming from a solvent in which neutralization was carried out), which can be explained by effective transesterification catalyzed by a strong acid. In contrast, in the latter case, the transesterification process is significantly limited; therefore, the dominant series of linear chains are terminated with benzyl ester. Further, a more detailed analysis of MALDI TOF spectra, including their modeling within different models, was discussed in SI.

To summarize this part of the work, one can conclude that we have managed to synthesize well-defined PGBLs in a wide range of an absolute M_n (usually 2.8–15.0, and also with M_n up to 30.3 kg/mol), narrow/moderate dispersity (usually $Đ$ = 1.12–1.89 and even 3.2) and high yields (usually 0.15–0.69 g_{PGBL}/g_{GBL}). GPC and MALDI-TOF results revealed that at p = 1000 MPa, elongation of the reaction time, implementation of higher catalyst concentration, or lower polymerization temperature contribute to the production of polymers with a higher amount of cyclic structures. Herein, it should be reminded that TBD has been used before by Hong et al. for the ambient pressure, low-temperature polymerization (T = 233-223 K) of γ-GBL. They reported that after 24 h, PGBL of M_n = 5.55–6.15 kg/mol were obtained with an efficiency of 17–33% [18]. Our reference high pressure experiments clearly demonstrated that applying the external catalytic force (elevated pressure) allowed us to obtain polymers of higher molecular weight, still narrow dispersity and higher yield in a much shorter time (1–3 h). Interestingly, in the case of data reported by some of us for water-initiated pressure-assisted TBD-catalyzed ROP of ε-caprolactone, we did not observe any significant influence of pressure on the progress of ROP as well as properties of recovered polymers [45]. Herein, we should also refer our result to the recent progress in the organocatalyzed polymerization of GBL. As previously mentioned, GBL ROP has been mediated by different organocatalysts with greater or lower effectiveness. Among them, the most effective turned out to be urea [30]/phosphazene [25] based compounds (or their combination) [28,29] yielding polymers with higher molecular weights, reaching even up to 80.4 kg/mol (relative to PS standards) [29], when produced using urea/CTPB binary catalyst at ultra-low temperatures (223 K). Moreover, in such a system, the dispersity of produced PGBLs was significantly higher as molecular weight increased, reaching $Đ$ = 1.97 in the case of the highest determined M_n = 80.4 kg/mol [29].

To further characterize obtained polymers, we measured the basic thermal, rheological and toxicity properties and the ability to serve as cell culture supports of the produced PGBL. Representative DSC thermograms obtained for selected polymer characterized by different topologies (varying content of linear vs cyclic polymers) are shown in Fig. S12 (see SI file).

DSC curve recorded for the polymer that contains the highest amount of cyclic macromolecules (sample S28) exhibits the two separated melting temperatures, T_m, see dashed line in Fig. S12. According to the previous study on PGBL homopolymers [18], T_m located at lower ($T_m \sim$ 323 K) and higher temperature range, $T_m \sim$ 333 K, can be assigned to melting temperatures of cyclic and linear polymers, respectively. However, as cyclic macromolecules' content decreases in the examined material, it seems that the endothermic peak located at $T_m \sim$323 K shifts to higher temperatures resulting in a bimodal endothermic peak (dotted line in Fig. S12). On the other hand, samples characterized by a negligible amount of cyclic polymers displayed only one melting temperature at $T_m \sim$333 K; see the solid line in Fig. S12.

Furthermore, to elucidate the impact of topology and its composition (copolymers with lactide), we also performed mechanical measurements of the produced materials. The first selected representative samples were characterized by similar absolute molecular weights but differing in cyclic moieties' concentration as revealed by MALDI-TOF analysis. Specifically, the first sample - sample 8, is characterized by much smaller cyclic products than the second one (sample 17). The differences in the samples' topology mentioned above result from preparation at various thermodynamic conditions, e.g., different temperature, initial catalyst concentration and/or reaction time. Moreover, it has to be pointed out that both samples were prepared under the same high pressure of p = 1000 MPa. Both materials have been placed between the rheometer fixtures and heated up to T = 353 K. At this particular temperature, the samples were liquefied, and then the gap was set. Next, their complex viscosity was examined in the wide frequency range (1–100 rad/s) for temperatures from T = 353 K to T = 313 K with a step of 10 K. The comparison of the obtained complex viscosity curves as a function of frequency is presented in Fig. 6a.

As can be seen with decreasing the temperature, the polymers become more viscous. The viscosity values were determined from the plateau regions and plotted versus the inverse of temperature in panel b of Fig. 6. To parameterize the obtained η(T) dependences, we employed the Vogel-Fulcher-Tamman (VFT) equation that is defined as follows:

$$\boldsymbol{log_{10}\eta(T) = log_{10}\eta_{\infty} + \frac{B}{T - T_0}}. \quad (1)$$

where T is temperature and η_∞, $B = DT_0$, T_0 are parameters obtained by fitting the VFT equation to experimental viscosity data. The values of η_∞, B and T_0 are equal to −1.33 ± 0.15, 1178 ± 83, 179 ± 5 and −3.20 ± 0.09, 1464 ± 75, 161 ± 3 for samples 17 and 8, respectively. By comparing obtained dependencies, one can easily conclude that the polymer's viscosity increases with an increasing amount of cyclic products. In other words, the viscosity of sample 17 is 1.5 order of magnitude greater than that of sample 8. This result is in contrast to a previously reported trend by Hong et al. [18], which found cyclic polymers characterized by lower viscosity in comparison to the linear counterparts of similar molecular weight. Hence, the discrepancy between our data and that published by Hong et al. could be related to a probably higher molecular weight of the cyclic moieties with respect to the linear ones. Nevertheless, it has to be pointed out that despite the observed differences in the polymers' viscosity, the tendency of the sample toward re-crystallization has not been changed. Both polymers re-crystallize at the same temperature conditions, i.e., during the stabilization of temperature equal to T = 313 K. This result is reflected by the visibility of a drastic viscosity increase in panel a of Fig. 6.

The observed differences in polymers' viscosity with a small and large number of cyclic products motivated us to investigate how this parameter change when the second – amorphous – polymer PLLA segment has been incorporated into copolymer structure via atmospheric-pressure TBD-catalyzed chain-extension experiment (see SI). The comparison of viscosity and stability of polymer sample 8 and its copolymer (i.e., PGBL-bl-PLA) is presented in Fig. 7.

Particularly noteworthy is that despite the presence of an additional polymeric segment, the viscosity of sample 8 was not as much changed as in the case of increasing content of cyclic moieties. However, polymeric chain modification had a higher impact on re-crystallization tendency. Namely, the re-crystallization of PGBL-bl-PLA was noted at a lower temperature than in the case of both sample 8 and sample 17. This result might indicate that the added polymeric segment improves the physical stability of the investigated polymers. This finding may have strong implications for further processing, shaping of the copolymers.

As a final part of our work, we performed cytotoxicity and cell proliferation studies on the structurally, topologically and morphologically different PGBLs samples. Note that measurements were conducted on the previously prepared PGBL-based films. It should be emphasized that produced films significantly differed in, e.g., their fragility, foil formation ability resulting from different content of cyclic topologies. It is also worth noting that films prepared from PGBL of higher dispersity (higher content of cycles) were characterized by lower fragility/higher flexibility than those based on polymers of much lower dispersity, which probably resulted from the highly plasticizing effect of both low molecular weight and cyclic fractions.

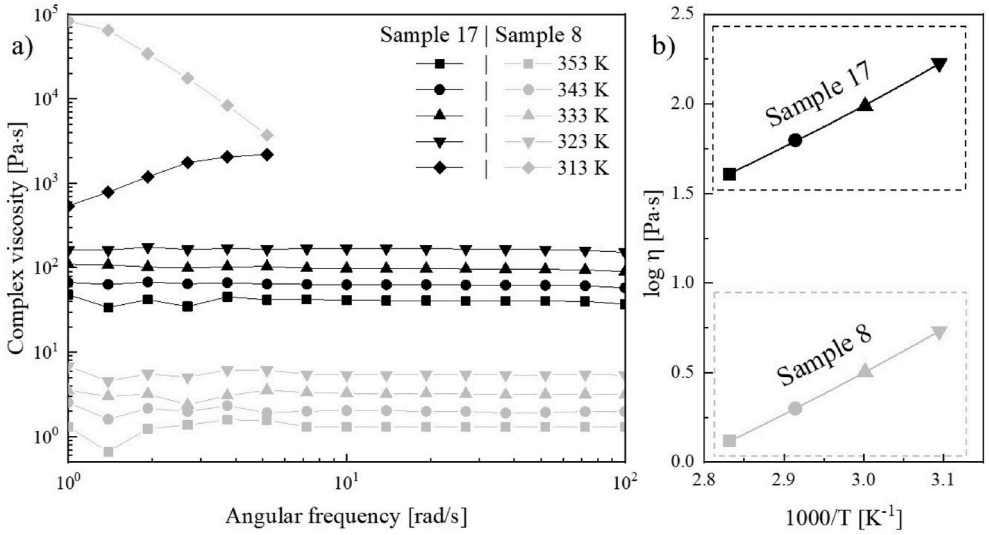

Fig. 6. (a) Temperature sweep rheological data showing complex viscosity as a function of the frequency of sample 8 (grey data) and sample 17 (black data) polymer; (b) Comparison of the temperature dependences of complex viscosity of sample 8 (grey data) and sample 17 (black data) polymer. The solid lines correspond to VFT fits.

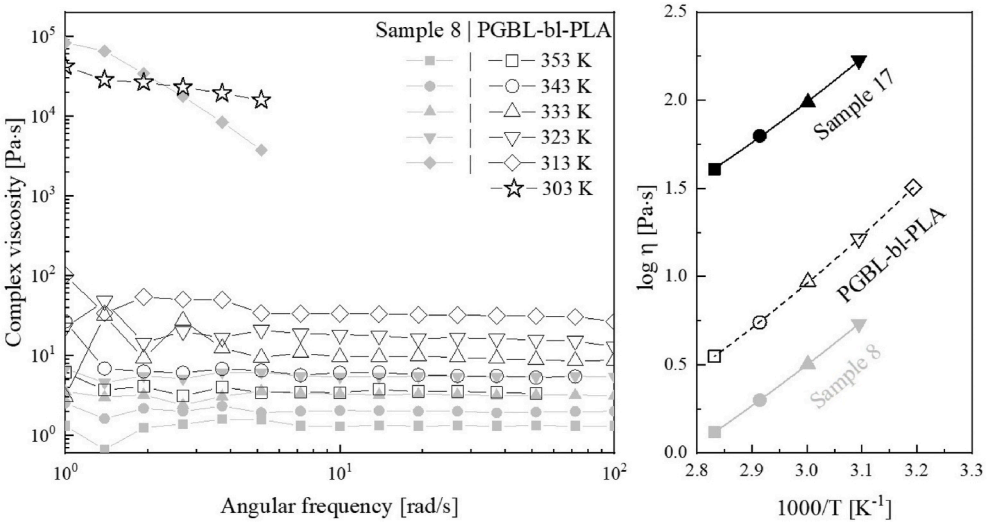

Fig. 7. (a) Temperature sweep rheological data showing complex viscosity as a function of the frequency of sample 8 (filled grey data) and a sample of PGBL-bl-PLA (empty black data) polymer; (b) Comparison of the temperature dependences of complex viscosity of sample 17 (filled black data), sample 8 (filled grey data), and a sample of PGBL-bl-PLA (empty black polymer). The solid lines correspond to VFT fits.

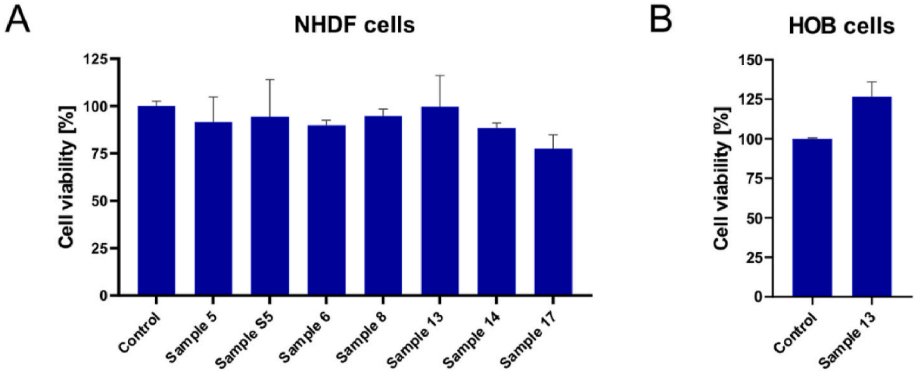

Fig. 8. Cell viability seeded onto PGBL samples.

It is worth noting that cytotoxicity analysis was performed using the MTS assay test while the cell's ability to proliferation was determined by measuring the absorbance of the formazan, an agent produced only in metabolically active cells. The experimental model was based on normal human dermal fibroblasts, a popular substituent of expensive in vivo experiments. This approach is a common simple screening system for testing the toxicity. Selected experimental models allowed determining the potential usage of the tested materials in a broad field of applications, from biocompatible implants or drug carriers to everyday items. Results indicate that seven of the tested PGBL-based materials showed no cytotoxic effect towards the NHDF cell line. Fraction of the proliferating cells excess 75% for sample 17 ($M_n = 10.4$ kg/mol; $Đ = 1.89$) and 80% for sample 14 ($M_n = 7.8$ kg/mol, $Đ = 1.13$). For the rest of the tested materials, the living population of cells was comparable to the control. The best result was achieved for sample 13 ($M_n = 7.5$ kg/mol; $Đ = 1.43$), for which we conducted an additional experiment with the human osteoblasts cell line. As is shown in Fig. 8b fraction of the proliferating osteoblasts exceeds the number of cells growing on the commercial surface.

Moreover, we stained cells with CellTracker Green CMFDA, which visualizes the whole cellular surface. Images depicted in Fig. 9 indicate that tested materials possess good attachment properties.

It seems that the worst results among the tested samples, but slightly different from the others, were observed for the PGBL with the highest M_n, $Đ$ and the content of cyclic forms. Other samples were characterized by lower M_n ranging from 5.4 to 7.0 kg/mol and low/moderate dispersity ($Đ = 1.13$–1.68) and had a much lower content of cycles than sample 17. Therefore, polymers with such properties show better cell-cell interactions, cell migration and proliferation. However, it should be kept in mind that the biodegradable films' particular mechanical properties are only one of the factors qualifying polymeric materials as good cell culture media (e.g., scaffolds). Other important factors are assigned to scaffold features such as surface topography and chemistry, i.e., wettability, softness, stiffness and roughness and microstructure, i.e., porosity, pore size or pore shape. It is worth noting that scaffold pore sizes play an essential role in oxygen and nutrient diffusion and waste removal and, therefore, strongly influence cell adhesion and cell-cell interactions. Literature data also showed that the osteoblasts attached and proliferated more effectively on the rough PLLA-based surface than the smooth one [54]. With this finding kept in mind, we looked deeper into the formed PGBL-based films' surface and performed SEM analysis (see Figs. S13-S15, SI). The morphology attained for the neat PGBL-based films shows a smooth and homogeneous surface with some microcracks and large filaments. It should also be stressed that tested films only slightly differed in roughness, which was higher in polymers with a higher content of cyclic forms. Perhaps better properties could be observed in the case of electrospun fibrous scaffolds. To conclude, toxicity and proliferation tests described above clearly indicated that PGBL is a non-toxic, biocompatible material that can be successfully used in biomedical applications. What is more, the cyclic/linear composition in PGBL slightly influences the proliferation ability, cell attachment, and properties of the cell culture supports.

4. Conclusions

In this paper, we have studied TBD-supported polymerization of GBL's at various thermodynamic conditions ($T = 233$–268 K and $p = 0.1$–1000 MPa). The reactions performed at different mixture compositions yielded polymers of '*pseudo-living*' character with moderate to high molecular weight (M_n up to 30.3 kg/mol) and low to moderate dispersity ($Đ = 1.12$–1.89). What is more, referring to the data presented by Hong et al., it was found that applying elevated pressure allowed us to *i)* significantly reduce the time of reaction, *ii)* increase the yield of produced PGBL and *iii)* synthesize polymers of narrow dispersity and higher molecular weights with respect to the polymerization carried out at $p = 0.1$ MPa. Further, more detailed MALDI-TOF and GPC measurements demonstrated that by elongation of the reaction time, an increase of the catalyst concentration or lowering the temperature, one can easily tune the properties of the obtained polymers, e.g., increase the number of macrocycles and dispersity. Moreover, after rheological studies, we noticed that polymer's viscosity increased with an increasing amount of cyclic products and the chain structure modification shows a strong impact on re-crystallization tendency. This finding may be crucial considering potential application since it opens many ways of further processing and shaping the highly biodegradable copolymers. Furthermore, the toxicity and proliferation tests clearly proved that PGBL is a

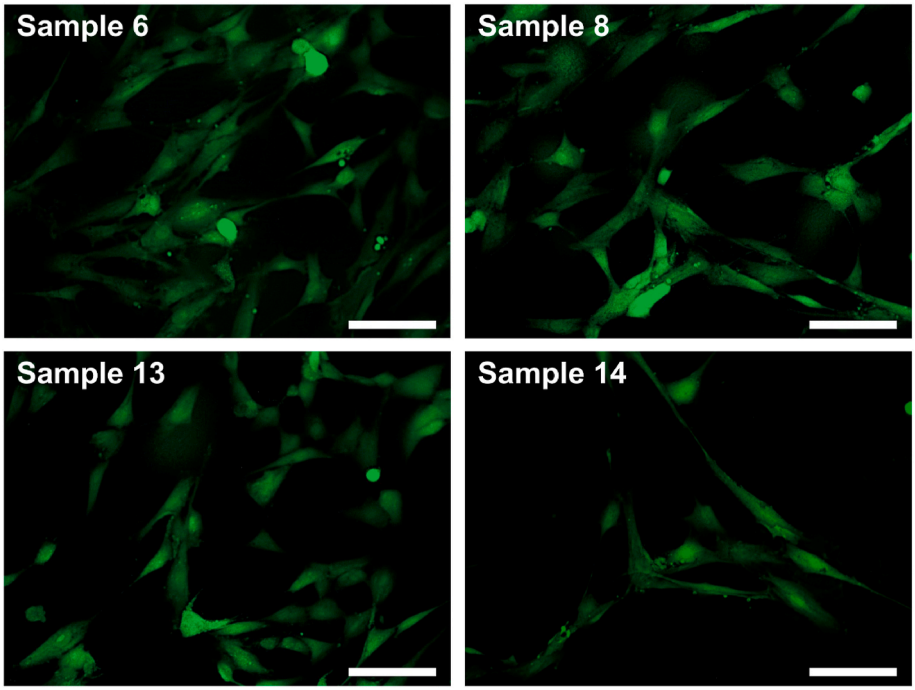

Fig. 9. Cell morphology of fibroblasts after seeded onto PGBL samples. Scale bars = 50 μm.

non-toxic and biocompatible material that can be successfully used in biomedical applications.

CRediT authorship contribution statement

Roksana Bernat: Conceptualization, Methodology, Formal analysis, Investigation, Resources, Writing – original draft, Writing – review & editing, Visualization, Funding acquisition. **Paulina Maksym:** Conceptualization, Methodology, Formal analysis, Investigation, Resources, Writing – original draft, Writing – review & editing, Visualization, Funding acquisition. **Magdalena Tarnacka:** Formal analysis, Resources, Investigation. **Kajetan Koperwas:** Formal analysis, Investigation. **Justyna Knapik-Kowalczuk:** Formal analysis, Investigation. **Katarzyna Malarz:** Formal analysis, Investigation. **Anna Mrozek-Wilczkiewicz:** Formal analysis, Investigation. **Andrzej Dzienia:** Formal analysis, Investigation. **Tadeusz Biela:** Formal analysis, Investigation. **Roman Turczyn:** Formal analysis, Investigation. **Luiza Orszulak:** Investigation, Resources. **Barbara Hachuła:** Formal analysis, Investigation. **Marian Paluch:** Project administration, Supervision. **Kamil Kamiński:** Project administration, Supervision, Funding acquisition.

Declaration of competing interest

The authors declare that they have no known competing financial interests or personal relationships that could have appeared to influence the work reported in this paper.

Acknowledgements

R. B. and P. M. are thankful for financial support from the Polish National Science Centre within the SONATA project (DEC-2018/31/D/ST5/03464). K. K. acknowledges the financial assistance from the Polish National Science Centre within the SONATA BIS 5 project (DEC-2015/18/E/ST4/00320). A.D. is grateful for the financial support from the Foundation for Polish Science within the START project.

Appendix A. Supplementary data

Supplementary data to this article can be found online at https://doi.org/10.1016/j.polymer.2021.124166.

References

[1] S.J. Huang, Biodegradation, in: G. Allen, J.C. Bevington (Eds.), Compr. Polym. Sci. Suppl. (1989) 597–606, https://doi.org/10.1016/B978-0-08-096701-1.00201-9.
[2] I. Vroman, L. Tighzert, Biodegradable polymers, Materials (Basel) 2 (2009) 307–344, https://doi.org/10.3390/ma2020307.
[3] R.P. Brannigan, A.P. Dove, Synthesis, properties and biomedical applications of hydrolytically degradable materials based on aliphatic polyesters and polycarbonates, Biomater. Sci. 5 (2017) 9–21, https://doi.org/10.1039/c6bm00584e.
[4] Y. Qin, A brief description of textile fibers, Med. Text. Mater. (2016) 23–42, https://doi.org/10.1016/b978-0-08-100618-4.00003-0.
[5] R. Francis, N. Joy, A. Sivadas, Synthetic biodegradable polymers for medical and clinical applications, biomed, Appl. Polym. Mater. Compos. (2016) 361–382, https://doi.org/10.1002/9783527690916.ch12.
[6] M.A. Woodruff, D.W. Hutmacher, The return of a forgotten polymer - polycaprolactone in the 21st century, Prog. Polym. Sci. 35 (2010) 1217–1256, https://doi.org/10.1016/j.progpolymsci.2010.04.002.
[7] S. Slomkowski, Biodegradable polyesters for tissue engineering, Macromol. Symp. 253 (2007) 47–58, https://doi.org/10.1002/masy.200750706.
[8] Y. Bu, J. Ma, J. Bei, S. Wang, Surface modification of aliphatic polyester to enhance biocompatibility, Front. Bioeng. Biotechnol. 7 (2019) 1–10, https://doi.org/10.3389/fbioe.2019.00098.
[9] J. Zhan, A. Singh, Z. Zhang, L. Huang, J.H. Elisseeff, Multifunctional aliphatic polyester nanofibers for tissue engineering, Biomatter 2 (2012) 202–212, https://doi.org/10.4161/biom.22723.
[10] I. Manavitehrani, A. Fathi, H. Badr, S. Daly, A.N. Shirazi, F. Dehghani, Biomedical applications of biodegradable polyesters, Polymers (Basel) 8 (2016), https://doi.org/10.3390/polym8010020.
[11] G. Schwach, M. Vert, In vitro and in vivo degradation of lactic acid-based interference screws used in cruciate ligament reconstruction, Int. J. Biol. Macromol. 25 (1999) 283–291, https://doi.org/10.1016/S0141-8130(99)00043-4.
[12] K.S. TenHuisen, V.F. Janas, K.L. Cooper, D.W. Overaker, J.J. Yuan, Self-tapping resorbable two-piece bone screw, 2005. US6916321 B2.
[13] P.N. Patel, D. Jyoti Sen, K.G. Parmar, A.N. Nakum, M.N. Patel, P.R. Patel, V. R. Patel, Biodegradable polymers: an ecofriendly approach in newer millennium, Asian J. Biomed. Pharm. Sci. 1 (2011) 23–39.
[14] T. Moore, R. Adhikari, P. Gunatillake, Chemosynthesis of bioresorbable poly (γ-butyrolactone) by ring-opening polymerisation: a review, Biomaterials 26 (2005) 3771–3782, https://doi.org/10.1016/j.biomaterials.2004.10.002.
[15] D.P. Martin, S.F. Williams, Medical applications of poly-4-hydroxybutyrate: a strong flexible absorbable biomaterial, Biochem. Eng. J. 16 (2003) 97–105, https://doi.org/10.1016/S1369-703X(03)00040-8.
[16] L.S. Nair, C.T. Laurencin, Biodegradable polymers as biomaterials, Prog. Polym. Sci. 32 (2007) 762–798, https://doi.org/10.1016/j.progpolymsci.2007.05.017.
[17] M. Pluta, Morphology and properties of polylactide modified by thermal treatment, filling with layered silicates and plasticization, Polymer (Guildf) 45 (2004) 8239–8251, https://doi.org/10.1016/j.polymer.2004.09.057.
[18] M. Hong, E.Y.X. Chen, Completely recyclable biopolymers with linear and cyclic topologies via ring-opening polymerization of γ-butyrolactone, Nat. Chem. 8 (2016) 42–49, https://doi.org/10.1038/nchem.2391.
[19] M. Danko, J. Mosnázek, Ring-opening polymerization of γ-butyrolactone and its derivatives: a review, Polimery/Polymers 62 (2017) 272–282, https://doi.org/10.14314/polimery.2017.272.
[20] A. Duda, S. Penczek, Biopolymers, Wiley-VCH, Weinheim, 2002.
[21] E. Sugawara, H. Nikaido, Properties of AdeABC and AdeIJK efflux systems of Acinetobacter baumannii compared with those of the AcrAB-TolC system of Escherichia coli, Antimicrob. Agents Chemother. 58 (2014) 7250–7257, https://doi.org/10.1128/AAC.03728-14.
[22] A. Duda, T. Biela, J. Libiszowski, S. Penczek, P. Dubois, D. Mecerreyes, R. Jérôme, Block and random copolymers of ε-caprolactone, Polym. Degrad. Stabil. 59 (1998) 215–222, https://doi.org/10.1016/s0141-3910(97)00167-5.
[23] A. Duda, S. Penczek, P. Dubois, D. Mecerreyes, R. Jérôme, Oligomerization and copolymerization of γ-butyrolactone - a monomer known as unable to homopolymerize, 1: copolymerization with ε-caprolactone, Macromol. Chem. Phys. 197 (1996) 1273–1283, https://doi.org/10.1002/macp.1996.021970408.
[24] N. Zhao, C. Ren, H. Li, Y. Li, S. Liu, Z. Li, Selective ring-opening polymerization of non-strained γ-butyrolactone catalyzed by A cyclic trimeric phosphazene base, Angew. Chem. Int. Ed. 56 (2017) 12987–12990, https://doi.org/10.1002/anie.201707122.
[25] M. Hong, E.Y.X. Chen, Towards truly sustainable polymers: a metal-free recyclable polyester from biorenewable non-strained γ-butyrolactone, Angew. Chem. Int. Ed. 55 (2016) 4188–4193, https://doi.org/10.1002/anie.201601092.
[26] E.F. Connor, G.W. Nyce, M. Myers, A. Möck, J.L. Hedrick, First example of N-heterocyclic carbenes as catalysts for living polymerization: organocatalytic ring-opening polymerization of cyclic esters, J. Am. Chem. Soc. 124 (2002) 914–915, https://doi.org/10.1021/ja0173324.
[27] P. Walther, W. Frey, S. Naumann, Polarized olefins as enabling (co)catalysts for the polymerization of γ-butyrolactone, Polym. Chem. 9 (2018) 3674–3683, https://doi.org/10.1039/c8py00784e.
[28] C.J. Zhang, L.F. Hu, H.L. Wu, X.H. Cao, X.H. Zhang, Dual organocatalysts for highly active and selective synthesis of linear poly(γ-butyrolactone)s with high molecular weights, Macromolecules 51 (2018) 8705–8711, https://doi.org/10.1021/acs.macromol.8b01757.
[29] Y. Shen, Z. Zhao, Y. Li, S. Liu, F. Liu, Z. Li, A facile method to prepare high molecular weight bio-renewable poly(γ-butyrolactone) using a strong base/urea binary synergistic catalytic system, Polym. Chem. 10 (2019) 1231–1237, https://doi.org/10.1039/c8py01812j.
[30] L. Lin, D. Han, J. Qin, S. Wang, M. Xiao, L. Sun, Y. Meng, Nonstrained γ-butyrolactone to high-molecular-weight poly(γ-butyrolactone): facile bulk polymerization using economical ureas/alkoxides, Macromolecules 51 (2018) 9317–9322, https://doi.org/10.1021/acs.macromol.8b01860.
[31] W.N. Ottou, H. Sardon, D. Mecerreyes, J. Vignolle, D. Taton, Update and challenges in organo-mediated polymerization reactions, Prog. Polym. Sci. 56 (2016) 64–115, https://doi.org/10.1016/j.progpolymsci.2015.12.001.
[32] A.P. Dove, Organic catalysis for ring-opening polymerization, ACS Macro Lett. 1 (2012) 1409–1412, https://doi.org/10.1021/mz3005956.
[33] O. Coulembier, L. Mespouille, J.L. Hedrick, R.M. Waymouth, P. Dubois, Metal-free catalyzed ring-opening polymerization of β-lactones: synthesis of amphiphilic triblock copolymers based on poly(dimethylmalic acid), Macromolecules 39 (2006) 4001–4008, https://doi.org/10.1021/ma060552n.
[34] G.W. Nyce, T. Glauser, E.F. Connor, A. Möck, R.M. Waymouth, J.L. Hedrick, In situ generation of carbenes: a general and versatile platform for organocatalytic living polymerization, J. Am. Chem. Soc. 125 (2003) 3046–3056, https://doi.org/10.1021/ja021084+.
[35] J. Raynaud, W.N. Ottou, Y. Gnanou, D. Taton, Metal-free and solvent-free access to α,ω- heterodifunctionalized poly(propylene oxide)s by N-heterocyclic carbene-induced ring opening polymerization, Chem. Commun. 46 (2010) 3203–3205, https://doi.org/10.1039/b925415c.
[36] J. Raynaud, C. Absalon, Y. Gnanou, D. Taton, N-heterocyclic carbene-induced zwitterionic ring-opening polymerization of ethylene oxide and direct synthesis of α,ω-difunctionalized poly(ethylene oxide)s and poly(ethylene oxide)-b-poly (ε-caprolactone) block copolymers, J. Am. Chem. Soc. 131 (2009) 3201–3209, https://doi.org/10.1021/ja809246f.
[37] F. Nederberg, B.G.G. Lohmeijer, F. Leibfarth, R.C. Pratt, J. Choi, A.P. Dove, R. M. Waymouth, J.L. Hedrick, Organocatalytic ring opening polymerization of trimethylene carbonate, Biomacromolecules 8 (2007) 153–160, https://doi.org/10.1021/bm060795n.

[38] M. Rodriguez, S. Marrot, T. Kato, S. Stérin, E. Fleury, A. Baceiredo, Catalytic activity of N-heterocyclic carbenes in ring opening polymerization of cyclic siloxanes, J. Organomet. Chem. 692 (2007) 705–708, https://doi.org/10.1016/j.jorganchem.2006.10.006.
[39] B.G.G. Lohmeijer, G. Dubois, F. Leibfart, R.C. Pratt, F. Nederberg, A. Nelson, R. M. Waymouth, C. Wade, J.L. Hedrick, Organocatalytic living ring-opening polymerization of cyclic carbosiloxanes, Org. Lett. 8 (2006) 4683–4686, https://doi.org/10.1021/ol0614166.
[40] D.A. Culkin, S. Csihony, W. Jeong, A.C. Sentman, G.W. Nyce, A.P. Dove, R. Pratt, J. L. Hedrick, R.M. Waymouth, N-heterocyclic carbenes: organocatalysts for ROP of lactide, Polym. Prepr. (Am. Chem. Soc., Div. Polym. Chem.) 46 (2005) 710.
[41] P. Maksym, M. Tarnacka, R. Bernat, A. Dzienia, A. Szelwicka, B. Hachuła, A. Chrobok, M. Paluch, K. Kamiński, Light-mediated controlled and classical polymerizations of less-activated monomers under high-pressure conditions, Polym. Chem. 12 (2021) 4418–4427, https://doi.org/10.1039/D1PY00738F.
[42] M. Buback, A. Kuelpmann, C. Kurz, Termination kinetics of methyl acrylate and dodecyl acrylate free-radical homopolymerizations up to high pressure, Macromol. Chem. Phys. 203 (2002) 1065–1070, https://doi.org/10.1002/1521-3935(20020501)203:8<1065:AID-MACP1065>3.0.CO;2-F.
[43] M. Buback, F. D Kuchta, Variation of the propagation rate coefficient with pressure and temperature in the free-radical bulk polymerization of styrene, Macromol. Chem. Phys. 196 (1995) 1887–1898, https://doi.org/10.1002/macp.1995.021960608.
[44] A. Dzienia, P. Maksym, M. Tarnacka, I. Grudzka-Flak, S. Golba, A. Zięba, K. Kaminski, M. Paluch, High pressure water-initiated ring opening polymerization for the synthesis of well-defined α-hydroxy-ω-(carboxylic acid) polycaprolactones, Green Chem. 19 (2017) 3618–3627, https://doi.org/10.1039/c7gc01748k.
[45] A. Dzienia, P. Maksym, B. Hachuła, M. Tarnacka, T. Biela, S. Golba, A. Zięba, M. Chorążewski, K. Kaminski, M. Paluch, Studying the catalytic activity of DBU and TBD upon water-initiated ROP of ε-caprolactone under different thermodynamic conditions, Polym. Chem. 10 (2019) 6047–6061, https://doi.org/10.1039/c9py01134j.
[46] K. Yamashita, K. Yamamoto, J.I. Kadokawa, Acid-catalyzed ring-opening polymerization of γ-butyrolactone under high-pressure conditions, Chem. Lett. 43 (2014) 213–215, https://doi.org/10.1246/cl.130952.
[47] E. Zakharova, A.M. De Ilarduya, S. León, S. Muñoz-Guerra, Sugar-based bicyclic monomers for aliphatic polyesters: a comparative appraisal of acetalized alditols and isosorbide, Des. Monomers Polym. 20 (2017) 157–166, https://doi.org/10.1080/15685551.2016.1231038.
[48] C. Ji, S. Jie, P. Braunstein, B.G. Li, Fast and controlled ring-opening polymerization of δ-valerolactone catalyzed by benzoheterocyclic urea/MTBD catalysts, Catal. Sci. Technol. 10 (2020) 7555–7565, https://doi.org/10.1039/d0cy01551b.
[49] Q. Song, C. Pascouau, J. Zhao, G. Zhang, F. Peruch, S. Carlotti, Ring-opening polymerization of γ-lactones and copolymerization with other cyclic monomers, Prog. Polym. Sci. 110 (2020), https://doi.org/10.1016/j.progpolymsci.2020.101309.
[50] H. Alamri, J. Zhao, D. Pahovnik, N. Hadjichristidis, Phosphazene-catalyzed ring-opening polymerization of ε-caprolactone: influence of solvents and initiators, Polym. Chem. 5 (2014) 5471–5478, https://doi.org/10.1039/c4py00493k.
[51] S.H. Hansen, L. Nordholm, N-alkylation of tertiary aliphatic amines by chloroform, dichloromethane and 1,2-dichloroethane, J. Chromatogr. A 204 (1981) 97–101, https://doi.org/10.1016/S0021-9673(00)81643-X.
[52] Y. Yang, Solvent-Induced side reactions in peptide synthesis, side react, Pept. Synth (2016) 311–322, https://doi.org/10.1016/b978-0-12-801009-9.00014-8.
[53] Y. Shen, J. Zhang, N. Zhao, F. Liu, Z. Li, Preparation of biorenewable poly (γ-butyrolactone)-b-poly(l-lactide) diblock copolyesters via one-pot sequential metal-free ring-opening polymerization, Polym. Chem. 9 (2018) 2936–2941, https://doi.org/10.1039/c8py00389k.
[54] K. Hatano, H. Inoue, T. Kojo, T. Matsunaga, T. Tsujisawa, C. Uchiyama, Y. Uchida, Effect of surface roughness on proliferation and alkaline phosphatase expression of rat calvarial cells cultured on polystyrene, Bone 25 (1999) 439–445, https://doi.org/10.1016/S8756-3282(99)00192-1.